VI-Characterization of Soft Magnetic Materials by Driving Current or Voltage

Romano Giannetti[1], Mirko Marracci[2], Bernardo Tellini[2], and Carmine Zappacosta[2]

[1] *Universidad Pontificia Comillas de Madrid, c/ Aguilera 23, E-28015, Madrid, Spain, tel:+34 915422800, fax: +34 915 541 11 32, romano@dea.icai.upcomillas.es*
[2] *Università di Pisa, via Diotisalvi 2, I-56122, Pisa, Italy, tel:+39 0502217300, fax:+39 0502217333, mirko.marracci@dsea.unipi.it, bernardo.tellini@dsea.unipi.it, carmine.zappacosta@dsea.unipi.it*

***Abstract*-**We analyse the volt-amperometric (VI-) method for the characterization of minor loops of soft magnetic materials. By adopting several input signals and by operating at various frequencies in the 10 Hz – 10 kHz frequency range, we perform the measurement on a soft ferrite core. Through the use of two different measurement schemes, we control in the first case the voltage across– and in the second case the current through– the primary coil. Measurement results are reported and a comparison among the various techniques is provided throughout the paper.

***Topics*-**1. Direct Current and Low Frequency Measurements, 8. Waveform Analysis and Measurements, 12. Power and Energy Measurements

I. Introduction

The measurement of the primary current and of the secondary voltage is a classic method adopted for the magnetic characterization of soft magnetic materials [1], [2], [3]. Generally, the VI-technique has been adopted for the characterization of symmetric cycles [4], [5], and only recently appeared in the literature the possibility to extend the method to the measurement of asymmetric loops [6], [7], [8]. The main advantage of the sensorless VI-technique is the simplicity, even if the main drawback is its inability to operate at very low frequencies because of the high pass filter characteristic of the transformer. In this paper, we present both the capabilities and the main critical aspects of the sensorless approach for the measurement of asymmetric minor loops and of their accommodation.

II. VI-Method Approach

In Fig. 1, we show the two schemes adopted for controlling the voltage across and the current through the primary wrapping. The source v_s is an arbitrary signal generator which is connected to the primary circuit via a power amplifier implemented with a LF411 operational amplifier followed by a class AB power stage made with two complementary transistors TIP41C and TIP42C. We can derive the values of *H* and *B* via the Ampere's and Faraday-Neumann's laws through the measurement of the primary current and secondary voltage.

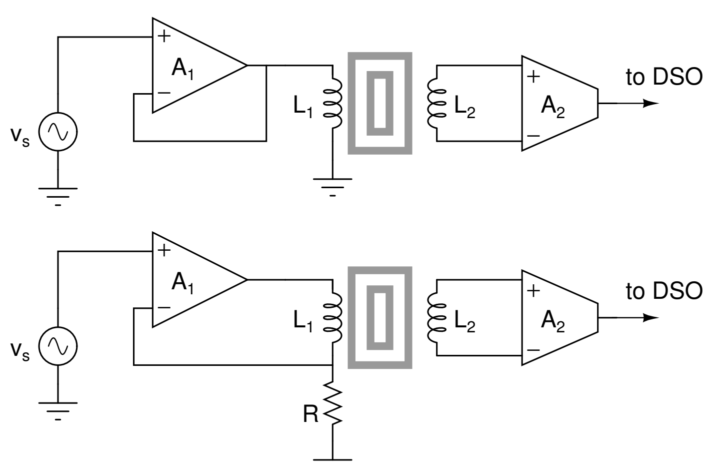

Figure 1. Upper plot: scheme adopted to drive the primary voltage. Lower plot: experimental setup to drive the primary current

Some of the main constraints encountered for imposing a well-known voltage across or current through a generic inductive load are summarized in Table 1:

Table 1. Some of the main critical points relevant to the voltage and current scheme of Fig. 1

V mode	I mode
$\omega L >> Z_{\text{int}} + R_w$	$\omega L << Z_{\text{int}} + R_w$
low frequency operation: strongly critical	low frequency operation: critical
discontinuity of B and voltage derivative: critical for the presence of parasitic effects	discontinuity of current derivative: critical for the presence of parasitic effects
estimation of B via integral calculation from the measured secondary voltage: not straightforward operation [7]	estimation of B via integral calculation from the measured secondary voltage: not straightforward operation [7]
voltage offset: critical for non periodic signals	voltage offset: critical for non periodic signals

where Z_{int} is the output impedance of the amplifier, R_w the winding ohmic resistance and L the equivalent inductance of the primary coil. In both modes, B is computed integrating the measured secondary voltage; such calculation of B requires also the knowledge of the initial magnetization state. Generally, we can solve this problem by strongly saturating the material or by reaching the demagnetisation state. The strong saturation ensures a single-valued $B - H$ relation and the wiping out of any past history. The null state can be accurately reached heating the sample over the Curie temperature and then by properly cooling it in the absence of magnetic fields [3] or, in a less accurate way, demagnetising the magnetic core by means of a series of diminishing in amplitude symmetric minor loops.

III. Results and Discussion

As for concerning the measurement of asymmetric minor loops, the voltage driving mode can be shown to be very critical. To explain this, let us assume to work with a linear $R - L$ load and to change the flux density in a continuous fashion from a sinusoidal waveform with zero average to a continuous value. From basic considerations of the circuit theory, since for a continuous value of B the corresponding applied voltage is zero, after the time t_0 the current will decay exponentially to zero. This is clearly shown in Fig. 2, where the expected induction field B, the voltage v proportional to the B–derivative and the current i calculated under steady-state conditions for a linear $R - L$ load are reported. In Fig. 2, we plot also the measured primary current and secondary voltage obtained for the same voltage input (solid lines – central and lower plots).

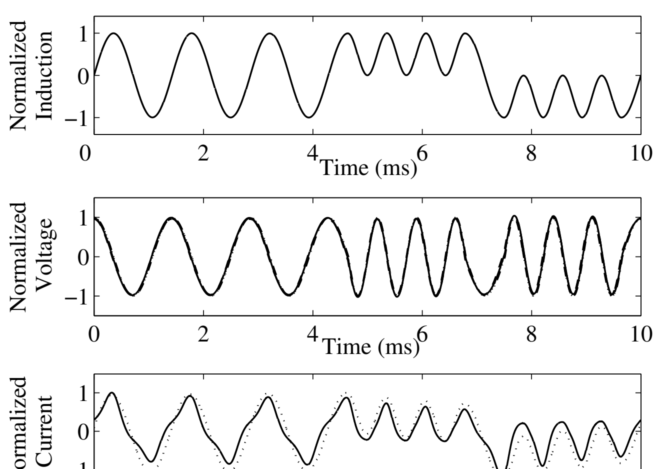

Figure 2. Upper plot: expected B behaviour; central plot: measured and simulated primary and secondary voltage (practically undistinguishable); lower plot: measured and simulated primary current. All plots are in normalized units.

We performed simulations choosing lumped parameter values estimated by the characteristics of the primary wrapping. Current results show clearly how the minor loops do not cycle between fixed extreme field values. In Fig. 3, we show the measured hysteresis cycles and the primary current obtained for an input voltage corresponding to an expected B signal (here not shown because of the available space) with minor cycles centered in $B = 0$. From such results, it is apparent how the minor cycles are not stabilized.

In Fig. 4, we show minor cycles centered on the *H*–axis and the relevant measured current. The accommodation is partially visible because dynamic effects are still present as can be argued by the detachment from the major loop of the branch connecting the major descending branch (MDB) to the minor loops and by the presence of negative values of the differential magnetic permeability $\partial B/\partial H$. To that respect, we recall that the condition $\partial B/\partial H > 0$ is a thermodynamic constraint for a static field [9].

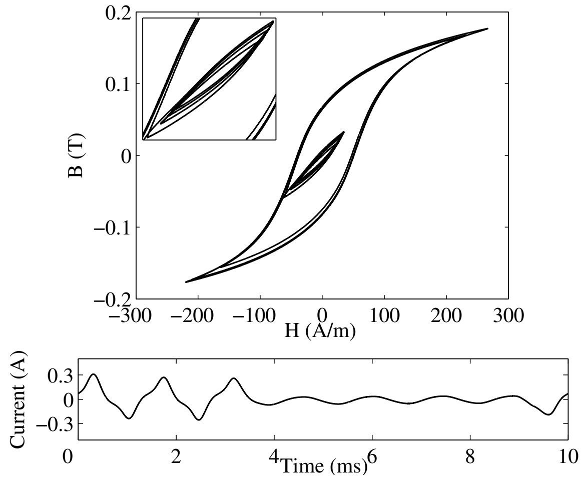

Figure 3. Measured hysteresis cycle and primary current (1 kHz)

As a final remark, attention must be given to avoid discontinuous voltage signal, i.e. *B* signals with discontinuous derivative. In such a case, the presence of parasitic elements would make more difficult a correct reconstruction of the minor cycles as shown in Fig. 5. Moreover, input signals with a not continuous first derivative are critical too for parasitic effects.

The current drive mode appears to be more suited for the observation of the accommodation phenomena. On the other hand this method is intrinsically more critical at relatively higher frequencies because of the condition: $\omega L << Z_{\text{int}} + R_w$. A detailed analysis of this method as well as of the possibility to measure asymmetric loops via a sensorless technique has been presented in [7]. Also in this case, care must be taken to avoid driving with current signals with discontinuous current derivative, in order to avoid behaviours analogous to that shown in Fig. 5. In Fig. 6, we show the measured hysteresis cycles and the corresponding primary current. Dynamic effects are practically not observable and minor loops cycle correctly between two well-controlled *H*– values. The accommodation is in this case observable [7], [8].

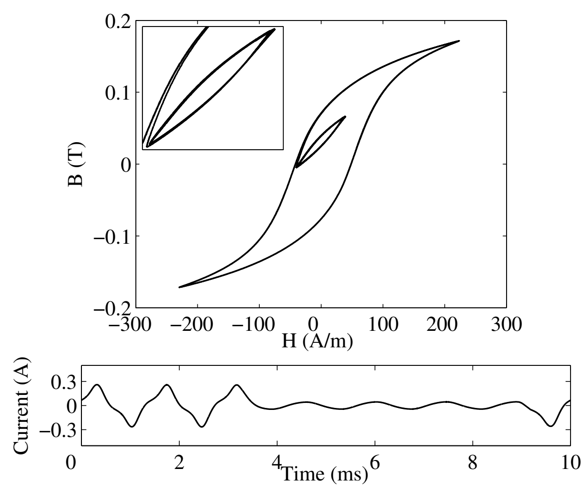

Figure 4. Measured hysteresis cycle and primary current; minor cycles centered on $H = 0$ (1 kHz)

A further test of the proposed techniques has been performed on a Fe-Si thin ribbon properly folded to form a closed ring. The physical dimensions are: 79 mm radius of the magnetic ring, 0.3 mm thickness of the lamination, 30 mm height of the lamination. The primary and secondary windings were formed by 40 turns each one.

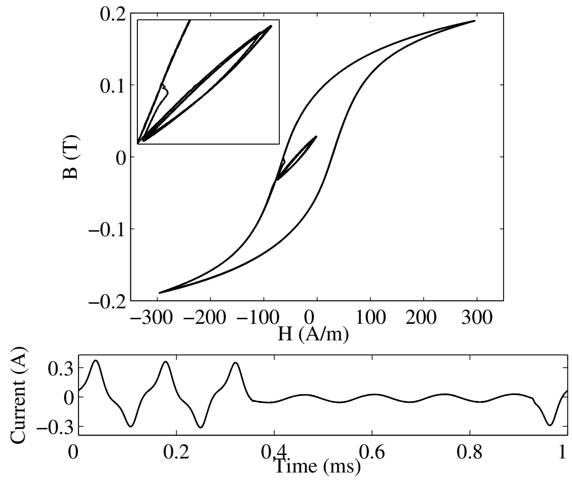

Figure 5. Measured hysteresis cycle and primary current (discontinuous voltage - 1 kHz)

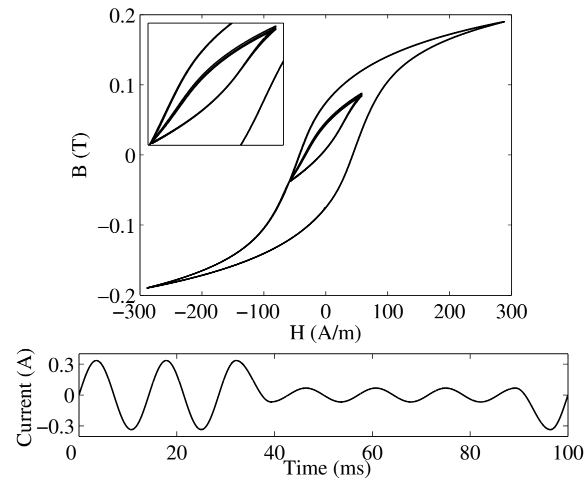

Figure 6. Measured hysteresis cycle and primary current (driving current mode - 1 kHz)

The V-mode was not applicable with such a setup. Indeed, in order to diminish the dynamic effects through the reduction of the operation frequency, the primary resistance value becomes larger than that of the inductive impedance. This leads to a voltage across the primary winding practically proportional to the primary current, as for the I-mode.

In Fig. 7, we show the measurement results obtained for the Fe-Si magnetic sample at 7 Hz – I-mode. It is possible to observe the dynamic effects through the detachment of the connecting branch between the major loop and the minor cycles. This data clearly show the necessity to reduce the operation frequency to properly measure accommodation.

In Fig. 8, we report data measured at 0.7 Hz – I-mode. It is possible to observe how dynamic effects are strongly reduced and the accommodation of the minor cycles is partially visible.

IV. Conclusions

We have presented a detailed performance analysis of a sensorless measurement procedure for the characterization of minor loops under periodic conditions, comparing the performances of two different strategies: driving the primary voltage (imposing dB/dt) or current (imposing H). From a theoretical point of view, the driving voltage mode has to be preferred at higher frequency and on the other way around the driving current scheme at lower frequency. This makes intrinsically the second measurement procedure more suited for the measurement of the accommodation phenomenon.

Results showed that discontinuity of the expected B, voltage and current derivative can be critical aspects because of parasitic effects.

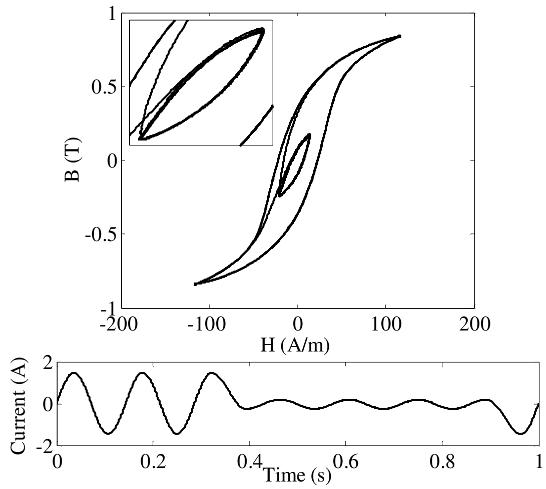

Figure 7. Measured hysteresis cycle and primary current for the Fe-Si magnetic sample (I-mode – 7 Hz)

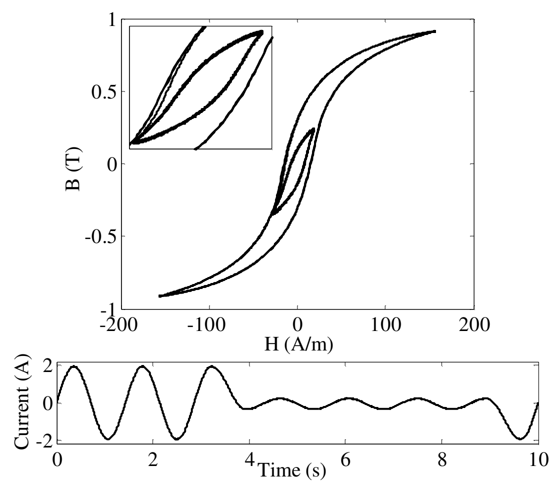

Figure 8. Measured hysteresis cycle and primary current for the Fe-Si magnetic sample (I-mode – 0.7 Hz)

References

[1] *IEEE Standard for Test Procedures for Magnetic Cores*, 1992. IEEE Std. 393-1991.

[2] *IEC 60404-2:1996 Magnetic materials - Part 2: Methods of measurement of the magnetic properties of electrical steel sheet and strip by means of an Epstein frame.*

[3] F. Fiorillo, "*Characterization and Measurement of Magnetic Materials (Electromagnetism)*," Elsevier Academic Press, 2004, Ch. 7.

[4] D. Grimaldi, L. Michaeli, A. Paumbo, "Automatic and Accurate Evaluation of the Parameters of a Magnetic Hysteresis Model," IEEE Trans. Instrum. Meas., vol. 49, No. 1, February 2000, pp. 154-160.

[5] A. J. Batista, J. C. S. Fagundes, and P. Viarouge, "An Automated Measurement System for Core Loss Characterization," IEEE Trans. Instrum. Meas., vol. 48, No. 2, April 1999, pp. 663-667.

[6] L. Cristaldi, A. Ferrero, M. Lazzeroni, A. P. Morando, "Sensorless Evaluation of Asymmetric Hysteresis Loops of Ferromagnetic Materials," IEEE Trans. Instrum. Meas., vol. 52, No. 3, June 2003, pp. 846-851.

[7] B. Tellini, R. Giannetti, S. Lizón-Martínez, "Sensorless Measurement Technique for Characterization of Magnetic Materials under Nonperiodic Conditions", to be published on *IEEE Trans. Instrum. Meas.*, vol. 57, no. 2. 2008.

[8] B. Tellini, R. Giannetti, S. Lizón-Martínez, and M. Marracci, "Accommodation Study via a Sensorless Measurement Technique," *Phys. B: Cond. Matter*, vol. 403, No. 2, Feb. 2008, p. 482-485.

[9] L. Landau and E. Lifshitz, "*Electrodynamics of Continuos Media*," 4th ed., Oxford, U.K.: Pergamon, 1981.